LBL--29522

DE91 011916

STUDY OF THE EFFECT OF REACTIVE ELEMENT ADDITION BY IMPLANTING METAL IONS IN A PRE-FORMED OXIDE LAYER

P. Y. Hou[*], *I. G. Brown*[*] *and J. Stringer*[**]

[*]Materials Science Division
Lawrence Berkeley Laboratory
University of California
Berkeley, CA 94720

[**]Electric Power Research Institute
Palo Alto, CA 94304

ABSTRACT

The influence of ion-implanted Y, Hf, Zr and Cr on the oxidation behavior of a Ni-25wt%Cr alloy at 1000°C has been investigated. The implantation dosage was 5×10^{16} ions/cm^2. Two methods of implantation have been used. One was to implant ions directly into a clean alloy surface; the other was to implant into an approximately 0.6 μm thick Cr_2O_3 layer formed at 1000°C on the alloy. In neither case did the Cr implantation show any beneficial effects. Implantations of Y, Hf and Zr produced all the reactive element effects, i.e. reduction in oxidation rate, elimination of base metal oxide formation and improvement in scale adhesion, only if the ions were initially implanted in the alloy. When the ions were implanted in a preformed oxide, the subsequent oxidation process was altered to the same degree as before, but the scale adhesion was not affected. Implications of these results to the mechanism of the reactive element effect are discussed.

This work was supported by the Electric Power Institute under contract No. RP 2261-1, through an agreement with the U. S. Department of Energy under Contract No. DE-AC03-76SF00098.

INTRODUCTION

Small amounts of elements forming stable oxides can have a beneficial effect on the high temperature oxidation behavior of alloys forming either Cr_2O_3 or Al_2O_3 protective external scales[1]. This is known as the Reactive Element Effect (REE). The principle manifestations of the REE in Cr_2O_3-forming alloys are i) an enhanced selective oxidation of chromium by either lowering the amount of Cr required to form a continuous protective Cr_2O_3 layer, or by reducing the formation of base metal containing oxides in the external scale; ii) a reduction in the growth rate of the chromia scale, particularly at temperatures above 900°C; iii) a change in transport mechanism through the scale from principally metal transport outward for alloys without the reactive element addition to principally oxygen transport inward and iv) an increase in the resistance of the scale to exfoliation on either thermal cycling or mechanical straining. For Al_2O_3-forming alloys, the only effect seems to be the enhanced spallation resistance of the alumina scales[2].

Although the benefits of the REE have been put to practical use for many years, mechanisms which lead to these phenomena are still under much debate. In this study, the REE is investigated by implanting the reactive elements into a Cr_2O_3-forming Ni-25wt%Cr alloy. Ion implantation has been a technique widely used recently for the study of the REE[3]. The technique permits comparison of oxidation behaviors between alloys which has a continued supply of the reactive element and alloys whose reactive element concentration is only incorporated in the surface region. This study, in particular, compares the effect of reactive element implantation into a clean alloy surface, as with conventional methods, and with implantations made into a pre-formed thin oxide layer.

EXPERIMENTAL METHODS

The Ni-25Cr alloy was prepared by induction melting and casting under an argon atmosphere, followed by a vacuum homogenization for 24 hours at 1100°C. The actual composition of Cr is very close to the nominal 25wt%. The average grain size was 1.5 mm x 0.4 mm x 0.3 mm. Specimens 15mm x 10mm x 1mm were cut from the center of the homogenized ingots, polished to a 600-grid SiC finish and thoroughly cleaned with alcohol before oxidation or implantation.

The ion-implantation was carried out using the metal vapor vacuum arc (MEVVA) high current metal ion source[4]. The source was operated in a pulsed mode with a mean ion energy of approximately 100 keV. Specimens to be implanted were mounted on a water-cooled holder suspended from a vertically moving shaft. Nominal dosage of $5\mathrm{x}10^{16}$ ions/cm^2 of Y, Hf, Zr or Cr were implanted. The number of beam pulses required to accumulate the required dose was calculated by adjusting the beam current prior to implantation. The actual doses were usually 20-30% lower than the nominal. Measured implantation depths ranged from 30 to 60 nm with a maximum concentration of 4-5 at% located about 20 nm from the surface. While most implantations were made into the surface of the Ni-25Cr alloy, a few were carried out into a pre-formed oxide layer on the alloy. The pre-oxidation was performed in dry oxygen at 1000°C for 10 minutes. The resulting oxide was a uniform, single-layered Cr_2O_3 with an approximate thickness of 0.6 µm.

Oxidation tests were carried out in dry oxygen at 1 atm. total pressure. Tracer experiments using ^{18}O were done on a few implanted specimens. For this purpose, specimens were first oxidized in flowing $^{16}O_2$ for 20 hours followed by slow cooling. Subsequent oxidation in $^{18}O_2$ was performed in a sealed quartz capsule, filled with a 95% $^{18}O_2$ enriched oxygen for another 4 hours.

RESULTS

The oxidation kinetics of the implanted and the unimplanted Ni-25Cr alloys are presented in Figure 1. The untreated Ni-25Cr initially oxidized to form a continuous

Cr_2O_3 scale. After about 5-10 hours, Ni-containing oxide nodules began to develop on the surface. The size and number of these nodules increased gradually with time. Oxidation of the pre-oxidized alloy resulted in a higher degree of Ni-oxide nodular formation, thus giving rise to a faster oxidation rate after the initial hours.

Implantation of Cr to the alloy or to the pre-formed oxide had no effect on the oxidation behavior of the Ni-25Cr alloy. This result indicated that any damages introduced by the implantation process could not be responsible for the effectiveness found in the Hf, Zr and Y cases. Similar to alloying additions of these reactive elements, a significant reduction in rate was observed with the Hf, Zr and Y implants, and the formation of Ni-containing oxides was also totally suppressed. This is true whether these metals were implanted in the alloy or in the pre-formed oxide, even when the pre-formed oxide layer was as thick as 2 μm.

Scale exfoliation, or spallation, often occurred during cooling of the alloy after high temperature oxidation. The degree of spallation is usually most conveniently presented by the weight of oxide loss. In Table 1, the spallation behavior of the tested alloys are summarized. It is seen that the reactive element implantations in the alloy not only affected the oxidation rate, but also prevented spallation. This is not true however, with implantations made in the pre-formed oxide layer. When comparing equal thickness of oxide scales, these specimens showed the same degree of spallation as the unimplanted Ni-25Cr.

Compositions of oxide scales formed on the Y-implanted specimens were studied using secondary ion mass spectroscopy (SIMS). The depth profiles through these scales are shown in Figure 2 and it is seen that the metal constituent of both scales was primarily Cr. The high Ni and Y concentration at the surface may be mainly due to surface enhancement common to SIMS analyses[5]. Position of the interface was estimated using a calibrated sputtering rate and the knowledge of the oxide thickness. The major difference found for the two depth profiles is seen to be the relative position of the Y peak with respect to the scale/metal interface. In (a), where the ions were implanted in the alloy, the Y concentrated near the surface. In (b), where Y implantation was made in a pre-formed oxide, the Y peak was found to be located in the middle of the scale. If one takes the implanted Y as a built-in, inert marker, these results suggest that the location of new oxide formation was slightly different in both cases.

In the case of implantations made in the alloy, the dominant transport process was oxygen inward diffusion, resulting in oxide growth at the scale/alloy interface, similar to that reported by other investigators[6]. With Y implanted into a pre-formed oxide layer however, steady state oxide growth seems to take place within the oxide, thus leaving the Y peak always located ahead of the pre-formed oxide layer. Results of the ^{18}O tracer study on this specimen is shown in Figure 3. If one takes the pre-formed oxide layer to be 0.6 μm thick, the majority of oxide growth can be seen to take place near the interface between the pre-formed oxide and the new oxide.

Morphologies of oxide scales formed on the Y-implanted specimens are shown in Figure 4. The scales shown here have been etched using a Br_2/MeOH solution to dissolve away the substrate. The cross-sectioned view in (a) and (b) showed that both of these scales are single-layered Cr_2O_3. In (a), where implantation was made in the alloy, the scale is almost single-grained with an irregular interface. The scale in (b), where implantation was made in the pre-formed oxide layer, consisted of fine grains, and had a much different appearance than that shown in (a). The underside of these scales are shown in (c) and (d) after totally dissolving the underlying alloy in Br_2/methanol. A comparison of these two micrographs showed that the oxide at the interface in the case of Y-implantation in the alloy had larger grains, but more importantly, the grains had a much more uniform structure and there were less voids.

DISCUSSIONS

Implantations of Y, Hf or Zr in the Ni-25Cr alloy or in a pre-formed Cr_2O_3 scale on the alloy all reduced the subsequent oxidation rate to the same degree as alloying additions of these metals. This clearly demonstrates that the effect of reactive element in reducing the oxidation rate involves incorporation of these elements in the oxide scale. In the case of Y implantations made in a pre-formed oxide, new oxide growth was found to take place near the original surface of the pre-formed oxide. A possible mechanism to explain this behavior is that the scale growth is controlled by a combination of Cr outward diffusion through most part of the pre-formed oxide, which was free from Y, and O inward diffusion through newly formed oxide, which has incorporated the implanted Y. It is not known however, exactly how the incorporation of Y or other reactive elements would change the transport mechanism in the scale. Although there have been suggestions[7] that segregations of Y to oxide grain boundaries could inhibit cation diffusion, thus allowing oxygen diffusion to dominate, the transport processes within these scales need further investigations before the effect of reactive element additions can be fully understood.

While the oxidation rates of reactive element implanted specimens were the same whether the implants were present in the alloy or in a pre-formed oxide, the spallation behavior of the oxides that formed was very different. The reason for this difference seems to lay in the scale growth process. In the latter case scale growth took place within the oxide. Golightly et al[8] have suggested that oxide growth within the scale can cause large compressive growth stresses which lead to scale buckling and failing. It seems possible that the slower oxidation rate, which might produce lower growth stresses, and this oxide growth within the scale counter acted each other to give rise to the observed spallation behavior which was unchanged from that of the untreated alloy. However, recent results[9] have shown that growth stresses are insignificant compared to thermal stresses in causing scale failure. The more important factor in deciding spallation behavior is the strength of the scale/alloy interface. A consequence of forming new oxides within the scale is that the scale/alloy interface remained the same as the original one which existed between the pre-formed oxide and the alloy. This is in contrast with implantations made in the alloy, where scale growth took place at the scale/alloy interface and good adhesion was found. These adherent scales had a more irregular interface with much more uniform structure and less voids, all of which are factors contributing to a stronger interface. Furthermore, the inwardly growing process would produce a cleaner interface by continually incorporating impurities, which may otherwise segregate to the interface to weaken it[10], into the scale.

CONCLUSIONS

Implantation of reactive elements in a pre-formed Cr_2O_3 scale on Ni-25wt%Cr alloy reduced the oxidation rate to the same degree as implantations made into the alloy, but while the latter showed excellent scale adhesion, the former had no effect. This behavior was found with Hf and Zr as well as with Y implants. It followed that the beneficial effect of reactive element addition in reducing the high temperature oxidation rate of Cr_2O_3 came from incorporation of the reactive elements in the oxide scale. This incorporation changed the predominant transport through the growing scale from Cr outward to O inward diffusion. With implantations made in the alloy, the majority of oxide growth took place at the scale/alloy interface, but with implantations made in the pre-formed oxide, it was at the interface between the new oxide and the pre-formed oxide . This growth process, which left the scale/metal interface the same as the untreated alloy, resulted in poor scale adhesion on these specimens.

ACKNOWLEDGEMENT

This work was supported by the Electric Power Institute under contract No. RP 2261-1, through an agreement with the U. S. Department of Energy under Contract No. DE-AC03-76SF00098.

REFERENCES

[1] L. B. Pfeil, U. K. Patent No. 574088, (1947)

[2] D. P. Whittle, and J. Stringer, Phil. Trans. Roy. Soc. London, A27 (1979) 309.

[3] M. J. Bennett and A. T. Tuson, Mat. Sci. and Eng., A116 (1989) 79.

[4] I. G. Brown, J. E. Galvin, R. A. Macgill and F. J. Paoloni, Rev. Sci. Instrum. 61 (1990) 577.

[5] R. J. Blattner and C. A. Evans, Jr., "Scanning Electron Microscopy IV", SEM Inc., Chicago, (1980) 55.

[6] C. M. Cotell, G. J. Yurek, R. J. Hussey, D. F. Mitchell and M. J. Graham, J. Electrochem. Soc., 134 (1987) 1871.

[7] K. Przybylski, A. J. Garratt-Reed and G. J. Yurek, J. Electrochem. Soc., 135 (1988) 509.

[8] P. Y. Hou and J. Stringer, to be published in Acta Met.

[9] F. A. Golightly, G. C. Wood and F. H. Stott, Oxid. Met., 14 (1980) 217.

[10] J. G. Smegill, A. W. Funkenbusch and N. S. Bornstein, Metall. Trans., 17A (1986) 923.

FIGURE CAPTIONS

Figure 1: Oxidation kinetics at 1000°C in 1 bar oxygen. The nominal dosage for all implantations were 5x10^{16} ions/cm^2. The pre-oxidation was carried out at 1000°C in oxygen for 10 minutes.

Figure 2: SIMS study of oxide scales formed at 1000°C for 24 hours on (a) 5x10^{16} Y-implanted Ni-25Cr, and (b) 5x10^{16} Y-implant in a pre-formed Cr_2O_3 on Ni-25Cr.

Figure 3: SIMS profiles of a Ni-25Cr specimen implanted with 5x10^{16} Y/cm^2 in a 0.6 µm pre-formed oxide, followed by oxidation in $^{16}O_2$ for 20 hours then in 95% enriched $^{18}O_2$ for 4 hours.

Figure 4: Comparison of scales formed at 1000°C for 50 hours with Y-implantation in metal ((a) and (c)) and with Y-implantation in oxide ((b) and (d)). (a) and (b) are cross-sections of the scales after deep etching using Br_2/MeOH. (c) and (d) are scale undersides.

Table 1: Summary of Oxidation and Spallation Behavior at 1000°C.

Oxidation Condition	Specimens	Weight Gain from Oxidation (mg/cm^2)	Weight of Spalled Oxide (mg/cm^2)
1000°C	Ni-25Cr	1.32±0.15	0.33±0.14
50 hours	Ni-25Cr-5x10^{16}Cr	2.05	0.13
	Ni-25Cr-5x10^{16}Y, Hf or Zr	0.43±0.10	0.01±0.01
	Ni-25Cr-5x10^{16}Y, Hf or Zr in oxide	0.35±0.07	0.13±0.05
8 hours	Ni-25Cr	0.52	0.14

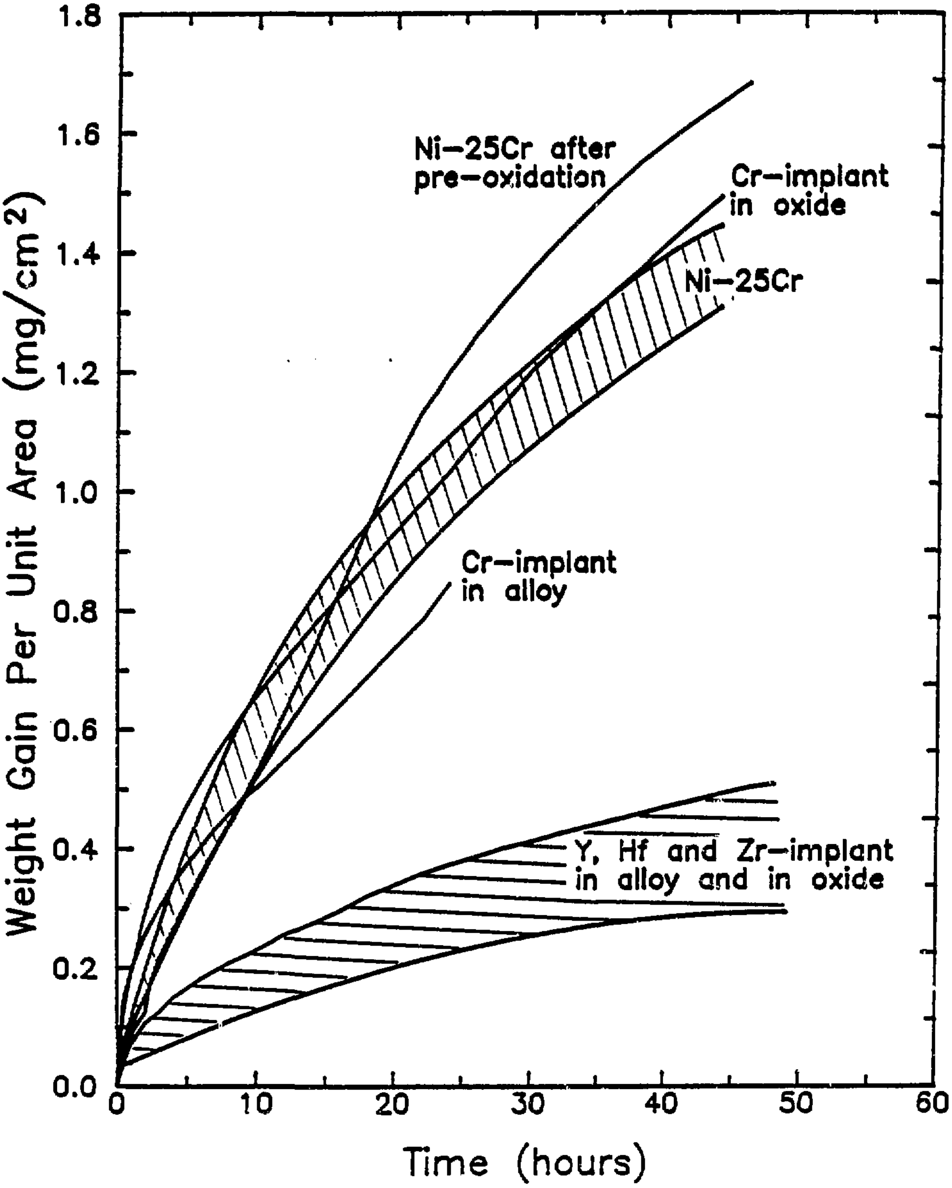

Weight Gain Per Unit Area (mg/cm²)
1.8
1.6
1.4
1.2
1.0
0.8
0.6
0.4
0.2
0.0
0
10
20
30
40
50
60
Time (hours)
Ni-25Cr after pre-oxidation
Cr-implant in oxide
Ni-25Cr
Cr-implant in alloy
Y, Hf and Zr-implant in alloy and in oxide

Figure 1

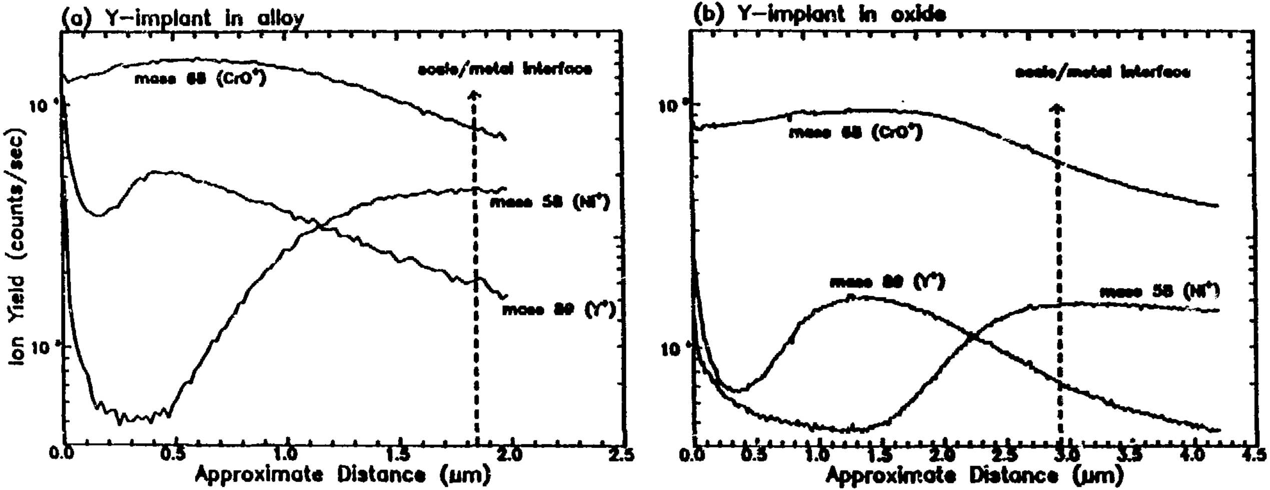
(a) Y–implant in alloy
scale/metal interface
mass 68 (CrO$^+$)
mass 58 (Ni$^+$)
mass 89 (Y$^+$)
10
10
Ion Yield (counts/sec)
0.0
0.5
1.0
1.5
2.0
2.5
Approximate Distance (µm)
(b) Y–implant in oxide
scale/metal interface
mass 68 (CrO$^+$)
mass 89 (Y$^+$)
mass 58 (Ni$^+$)
10
10
0.0
0.5
1.0
1.5
2.0
2.5
3.0
3.5
4.0
4.5
Approximate Distance (µm)

Figure 2

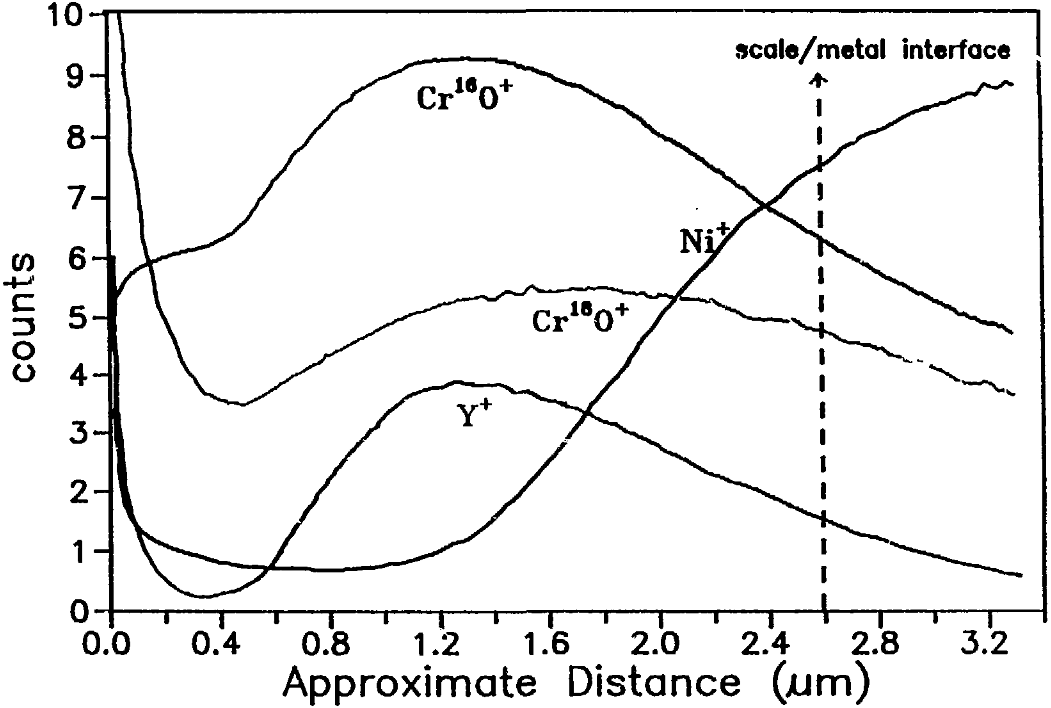
counts
10
9
8
7
6
5
4
3
2
1
0
0.0
0.4
0.8
1.2
1.6
2.0
2.4
2.8
3.2
Approximate Distance (μm)
scale/metal interface
$Cr^{16}O^+$
$Cr^{18}O^+$
Ni^+
Y^+

Figure 3

XBB 8611-9551-A (part A)

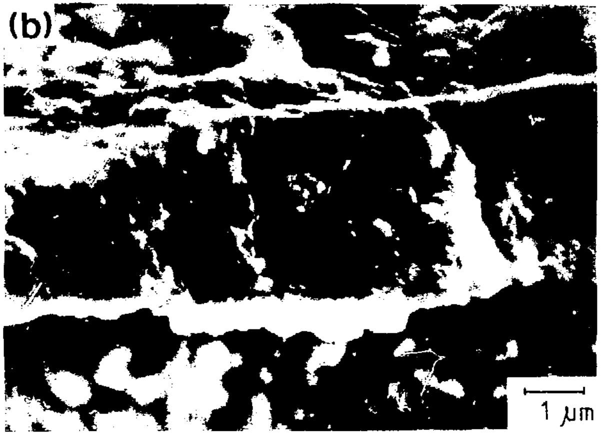

XBB 8611-9551-A (part C)

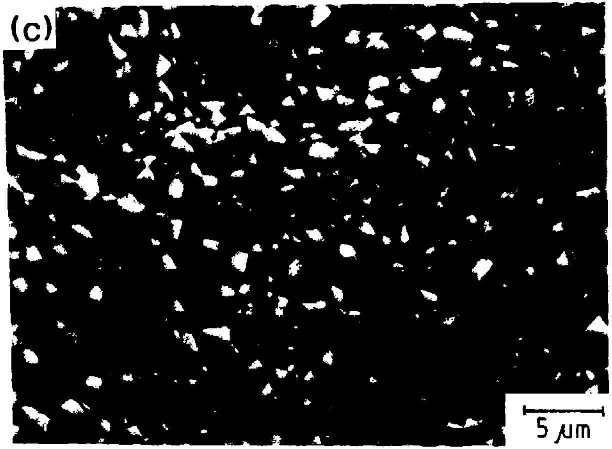

XBB 8611-9556 (part A)

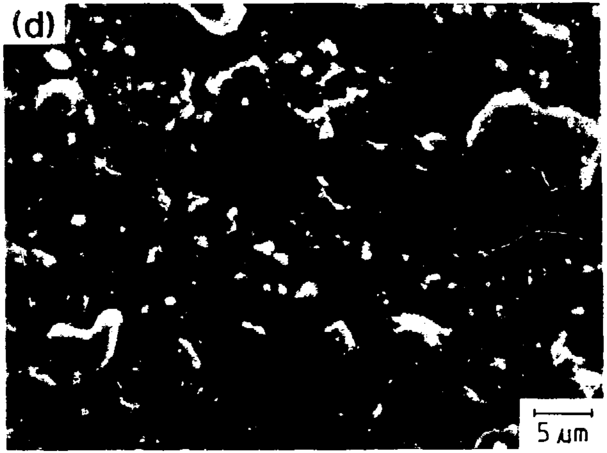

XBB 8611-9556 (part E cropped)